

Temperature effect on ideal shear strength of Al and Cu

Albert M. Iskandarov,^{1,2} Sergey V. Dmitriev,² and Yoshitaka Umeno¹

¹*Institute of Industrial Science, The University of Tokyo, 4-6-1 Komaba, Meguro-ku, Tokyo 153-8505, Japan*

²*Institute for Metals Superplasticity Problems, Russian Academy of Science, Khalturin St. 39, Ufa 450001, Russia*

(Received 19 June 2011; revised manuscript received 7 November 2011; published 27 December 2011)

According to Frenkel's estimation, at critical shear stress $\tau_c = G/2\pi$, where G is the shear modulus, plastic deformation or fracture is initiated even in defect-free materials. In the past few decades it was realized that, if material strength is probed at the nanometer scale, it can be close to the theoretical limit, τ_c . The weakening effect of the free surface and other factors has been discussed in the literature, but the effect of temperature on the ideal strength of metals has not been addressed thus far. In the present study, we perform molecular dynamics simulations to estimate the temperature effect on the ideal shear strength of two fcc metals, Al and Cu. Shear parallel to the close-packed (111) plane along the $[11\bar{2}]$ direction is studied at temperatures up to 800 K using embedded atom method potentials. At room temperature, the ideal shear strength of Al (Cu) is reduced by 25% (22%) compared to its value at 0 K. For both metals, the shear modulus, G , and the critical shear stress at which the stacking fault is formed, τ_c , decrease almost linearly with increasing temperature. The ratio G/τ_c linearly increases with increasing temperature, meaning that τ_c decreases with temperature faster than G . Critical shear strain, γ_c , also decreases with temperature, but in a nonlinear fashion. The combination of parameters, $G\gamma_c/\tau_c$, introduced by Ogata *et al.* as a generalization of Frenkel's formula, was found to be almost independent of temperature. We also discuss the simulation cell size effect and compare our results with the results of *ab initio* calculations and experimental data.

DOI: [10.1103/PhysRevB.84.224118](https://doi.org/10.1103/PhysRevB.84.224118)

PACS number(s): 05.45.Yv, 63.20.-e

I. INTRODUCTION

Defect-free crystalline materials have strength two to three orders of magnitude higher than conventional ones. In 1926, Frenkel offered a very simple estimation of the critical shear stress of an ideal crystal, $\tau_c \approx G/2\pi$, where G is the shear modulus.¹ Critical tensile stress is also used to characterize ideal strength of materials and it is of the same order of magnitude as the critical shear stress. The possibility of achieving strength close to the theoretical limit was demonstrated already in the early 1950s in the experiments on whiskers.² Nowadays, it is widely accepted that theoretical strength has not only fundamental but also practical importance, especially for nanomaterials, where the dislocations either are absent or cannot move or multiply.³ Materials exhibiting strength greater than 10% of the theoretical limit are often called ultrastrength materials.³

Recent experiments on mechanical loading of small-volume metals have shown that local stress can reach a significant fraction of the ideal strength. For instance, Wu *et al.*⁴ carried out a bending test of Au nanowires with a diameter of 40 nm using an atomic force microscope tip and measured yield stress to be 5.6 GPa, which is close to Frenkel's estimation. Minor *et al.*⁵ performed nanoindentation experiments of Al and estimated maximum shear stress of 2.3 GPa, compared to the theoretical strength of 2.84 GPa.⁶ Experiments on uniaxial compression of submicron- and nanopillars fabricated by a focused ion beam⁷⁻¹⁰ or by an alternative technique¹¹ demonstrate increase in the yield stress with decreasing sample diameter, d , according to the power law, $\sigma_y \sim d^{-n}$, when the samples have dislocations. On the other hand, samples free of initial dislocations have strength close to the theoretical limit and do not demonstrate the size effect.¹²⁻¹⁵ It has been found that even dislocation-free

grain boundaries in mechanically annealed nanometer-sized W bicrystals having nanometer dimensions are capable of withstanding extreme stresses close to the values of the theoretical strength of single crystals.¹⁶

The effect of a free surface on the ideal strength has been experimentally investigated by comparing the results of nanoindentation tests with those of the uniaxial compression of micropillars.¹⁷ It is known that, during nanoindentation, maximum shear stress is observed beneath the contact surface, resulting in homogeneous nucleation of dislocations.^{18,19} On the other hand, during compression of pillars, semi- or quarterloops can be nucleated at the sample surface or edge. In Mo-based alloys, it was found that the critical resolved shear stress for dislocation nucleation is equal to $G/8$ in single crystals under nanoindentation, while compression tests on micropillars reveal a critical shear stress of $G/26$.

Urged by these experimental results, many computational studies have been carried out to evaluate ideal strength of various crystals by means of *ab initio* and molecular dynamics approaches. While in the earlier works the aim was to calculate the ideal strength,²⁰ recently the interest of researchers shifted to the problem of why nanomaterials fail at stresses lower than the theoretical limit.

The effect of different factors on the ideal strength has been investigated numerically. For example, the weakening effect of twins and grain boundaries has been studied.^{21,22} A pronounced effect of crystallographic orientation on plastic deformation during nanoindentation of Al and Cu has been revealed.²³ In a series of works by Kolluri *et al.*, thin films of fcc metals, including Al and Cu, have been studied, ultrahigh strength has been demonstrated, and crystallographic orientation effects have been examined.²⁴⁻²⁶ The effect of normal stresses on the ideal shear strength in several covalent crystals has been studied.^{27,28} Effect of triaxial loading on

the ideal strength of six fcc crystals has been addressed.²⁹ The obtained results revealed that the compressive strengths increase (decrease) linearly with the transverse compressive (tensile) stresses. A free surface without notches does not noticeably affect the ideal strength of a two-dimensional model crystal,³⁰ in the presence of a notch, dislocations in a Cu single crystal are nucleated at stresses lower than the theoretical limit.³¹

The ideal strength calculated at 0 K sets the “athermal” limit of the local stress,³² while experiments are carried out at finite temperatures. Since thermal fluctuations at elevated temperature can assist structural instability or defect nucleation, it is important to understand the effect of temperature on the ideal strength. Recently, Zhu *et al.*³³ established a statistical model for dislocation nucleation stress and gave a function of the form $-T \ln T$. This model was applied to dislocation nucleation from surfaces in a Cu nanopillar under compression. At room temperature and strain rates used in experiments, the critical stress is evaluated to be only 30% of the ideal strength at 0 K. However, the model includes the effects of free surfaces and temperature. As was indicated in nanoindentation and punched micropillar experiments by Bei *et al.*,¹⁷ a wide range of critical stresses reported for various types of specimen indicates that the type of structure strongly affects the critical stress of instability. Thus one may naturally expect that the effect of temperature would depend on the structure.

To better understand the mechanism of crystal instability under loading, one should clarify how much the reduction in critical stress solely by the temperature effect is. It is therefore necessary to reveal the “ideal strength at finite temperature,” i.e., critical stress of mechanical instability of a perfect crystal at nonzero temperature. To the best of our knowledge, this problem has not been addressed for metals thus far.

In the present study, we use molecular dynamics (MD) simulations to investigate the temperature effect on the ideal shear strength (ISS) of single crystals of Al and Cu. Shear deformation in the $[11\bar{2}]$ direction on the (111) plane is considered because this is the direction of easiest shear for fcc metals. We select for our study Al and Cu as fcc metals with high and low stacking fault energies, respectively.

For six fcc crystals including Al and Cu, a simple way of estimating uniaxial tensile strength on the basis of theoretical shear strength was offered.³⁴ The results of the present study on ISS, with the help of their approach, can be used for estimation of the ideal tensile strength.

The instability problem for a single crystal can be addressed in terms of continuum mechanics by checking the positive definiteness of the elastic constant matrix at different strain levels³⁵ and different temperatures. However, we have chosen the most straightforward for an atomistic simulations way of stress-controlled loading until the instability event takes place with an abrupt structure transformation.

The paper is organized as follows. In Sec. II, we briefly describe the interatomic potentials used in our study and other simulation details. Then, in Sec. III A, our main numerical results are presented. Cell size effect is discussed in Sec. III B. Section IV concludes the paper.

II. SIMULATION DETAILS

A. Interatomic potentials

Our MD simulations of Al and Cu single crystals rely on potentials based on the embedded atom method (EAM). Boyer *et al.*³⁶ performed a comparison of shear deformation in Al and Cu using EAM potentials with the results of *ab initio* simulations based on the density functional theory (DFT). It was shown that the Mishin potential for Cu overestimates both ideal shear strength (2.91 GPa, while DFT gives 2.16 GPa) and critical strain, but qualitatively reproduces stress-strain relations. Moreover, the interplanar spacings during affine shear and stacking fault energy obtained by using this potential are in reasonably good agreement with those obtained by DFT. Therefore, we used the Mishin potential in calculations of Cu.

In contrast, Boyer *et al.* found the Mishin potential for Al³⁷ unsatisfactory, in the sense that it cannot accurately describe the evolution of distances between atomic planes during shear predicted by DFT calculations. This contradiction was explained by the more complicated process of charge redistribution during breaking and reforming bonds, caused by anisotropic electron density and directional bonding in Al. Besides, the stress-strain curve obtained with the use of the Mishin potential does not show nonlinearity, even at high strains, which does not make physical sense. Thus it was concluded that EAM potentials for Al reported by Mishin³⁷ were not suited for the present study.

Several alternative EAM potentials for Al have been developed and, in our investigation of ISS of Al, we used the EAM potential developed by Zope and Mishin.³⁸ Their potential correctly predicts the equilibrium crystal structure and accurately reproduces basic lattice properties. A reasonably good agreement with experimental data was reported for the stacking fault energy and energies of point defects.³⁸

B. Simulation procedure

Simulation cell vectors, \mathbf{a} , \mathbf{b} , and \mathbf{c} , are initially parallel to $[11\bar{2}]$, $[1\bar{1}0]$, and $[111]$ directions of the fcc lattice, respectively. The smallest sampled cell contains six atoms, which are located on three close-packed planes. To build larger cells and investigate the cell size effect on ISS, we used a replication of this cell in x , y , and z directions. For both metals, simulation cells containing from 48 up to 20250 atoms were used. The main results were obtained for the simulation cell with 1296 atoms. Justification of the choice of the simulation cell size will be given in Sec. III B.

We use engineering strain, $\gamma = \delta_x/L_z$, where δ_x is the displacement of simulation cell vector \mathbf{c} , which is initially along the $[11\bar{2}]$ direction, and L_z is the projection of the vector to the z direction [see Fig. 1(b)].

Temperature range from 0 K up to 800 K was sampled with a 100 K step for both metals and for each cell size.

Simulation started from equilibration of the crystal at a given temperature for 10 ps with a time step of 1 fs. Then, shear stress increasing with a constant rate of 50 MPa/ps was applied along $[11\bar{2}](111)$, while keeping other stress components equal to zero. The duration of the MD simulations

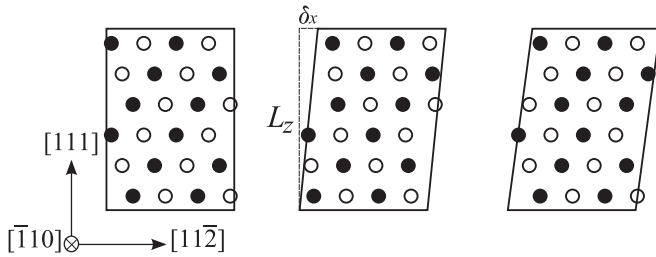


FIG. 1. Schematics of a simulation cell and atom positions. Atoms in different atomic planes parallel to the plane of figure are shown by open and filled circles. (a) $\gamma = 0$; (b) under shear deformation but before instability; (c) after stacking fault formation.

from zero to critical stress for different temperatures was typically in the range of 40 to 60 ps. The decrease in the stress increase rate may result in certain reduction in critical stress, especially at high temperatures, because triggering of a lattice instability event has a probabilistic nature. Nevertheless, we report the results with the above-mentioned stress increase rate, which is typical for MD simulations. Stress components were controlled using the Parinello-Rahman method.³⁹ Temperature was kept constant during the simulation by the velocity scaling method. Periodic boundary conditions were imposed in all three directions.

A note should be made on why we use the stress-controlled rather than strain-controlled loading. In the case of simple shear, for not small values of shear strain, nonzero compression stress acting normal to the close-packed planes appears and it affects the critical values of shear strain (or shear stress).²⁷ We have chosen an alternative way of stress-controlled loading aimed at analyzing critical shear stress at zero tension/compression stress normal to the close-packed atomic planes.

Because of the thermal atomic fluctuation, especially at high temperatures, results vary significantly from one simulation run to another, even for the same set of parameters. That is why we performed several runs (at least 10) for each structure and each set of parameters and analyzed the averaged values and dispersion. In our study, parameters of the Parinello-Rahman scheme were chosen in a way to minimize the role of fluctuations of the periodic cell. Technical details related to the accuracy control in our study are reported individually.⁴⁰

Two packages for MD simulations were used in our investigation, viz. MDSPASS developed in the University of Tokyo and LAMMPS.⁴¹ Having analyzed the influence of parameters of the simulators, we set their appropriate values; this resulted in a negligible difference in the results obtained by the two codes.

III. RESULTS AND DISCUSSION

A. Temperature effect on stress-strain curves, critical shear stress, and critical strain

Shear stress, τ , as a function of shear strain, γ , in Al and Cu is shown in Figs. 2(a) and 2(b), respectively. The results were obtained using a simulation cell containing $N = 1296$ atoms (see Sec. III B). Each figure shows a set of nine curves, which correspond to different temperatures. In the simulations

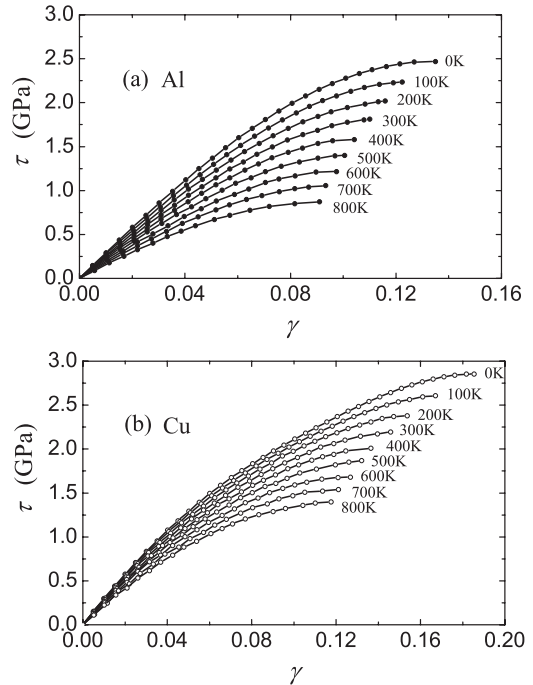


FIG. 2. Stress-strain curves of (a) Al and (b) Cu under stress-controlled loading by applying shear stress along $[11\bar{2}][111]$ at different temperatures. The number of atoms is 1296. The right end of each curve indicates the instability point.

at finite temperatures, τ and γ fluctuate over time, and thus in Fig. 2 we plot values averaged over several periods of fluctuation.

Shear elastic modulus at 0 K, calculated from the slope of the corresponding stress-strain curve at $\gamma = 0$, was found to be $G = 29.3$ GPa in Al and $G = 30.3$ GPa in Cu. The latter is in a good agreement with 31.0 GPa by DFT, while the former is larger than 25.4 GPa by DFT.⁴² For both metals, the slope of stress-strain curves at $\gamma = 0$ decreases with increasing temperature, meaning the reduction of the shear elastic modulus G . For instance, $G = 24.5$ GPa in Al and $G = 28.0$ GPa in Cu at 300 K.

Stress-strain curves terminate at the critical points, where shear strain suddenly increases at practically constant shear stress (the sudden increase in strain is not shown in Fig. 2). Within the studied temperature range, the mechanism of instability was the same, namely, stacking fault formation. It is seen that the increase in temperature causes the decrease of critical stress, τ_c , and critical strain, γ_c , in both metals. The critical shear stress of Al obtained at 0 K is $\tau_c^0 = 2.47$ GPa. This value is lower than 2.84 GPa evaluated by DFT calculations.^{6,36,42} The critical strain, $\gamma_c^0 = 0.135$, is about 35% lower than a DFT evaluation (0.2).⁶ Boyer *et al.*³⁶ reported that the Mishin potential gives critical stress of 3.12 GPa and critical strain of 0.15. In Cu, the critical stress at 0 K obtained using the Mishin potential is $\tau_c^0 = 2.85$ GPa, compared to 2.16 GPa by DFT. As for the critical strain, the obtained value is $\gamma_c^0 = 0.185$, more than 40% higher than that by DFT (0.130).

In Fig. 3, as a function of temperature normalized to the melting temperature, we present (a) critical shear stress normalized to its value at 0 K τ_c/τ_c^0 and (b) critical shear strain normalized to its value at 0 K, γ_c/γ_c^0 . The experimental

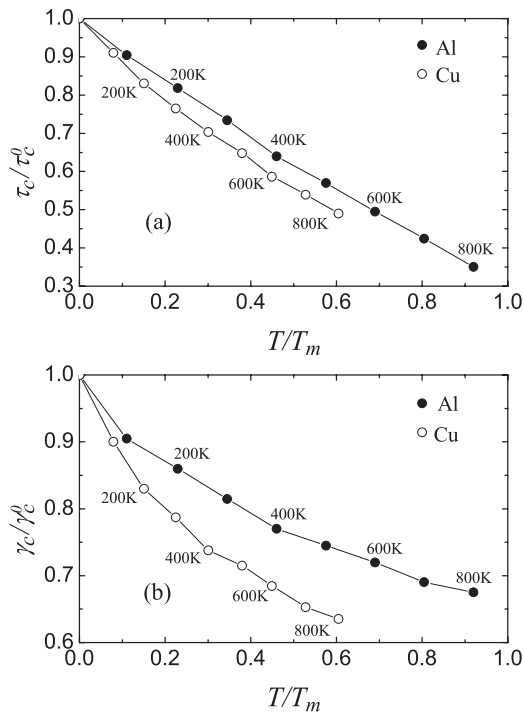


FIG. 3. Normalized critical shear stress (a) and critical shear strain (b) as functions of normalized temperature. Filled and open circles are for Al and Cu, respectively. Each point is the result of averaging over 10 numerical runs. Critical values at 0 K are as follows: for Al $\tau_c^0 = 2.47$ GPa, $\gamma_c^0 = 0.135$, and for Cu $\tau_c^0 = 2.85$ GPa, $\gamma_c^0 = 0.185$. We took for Al $T_m = 870$ K^{43,44} and for Cu $T_m = 1327$ K⁴⁵ (experimental values are $T_m = 933$ K for Al and $T_m = 1358$ K for Cu).

values of T_m of Al and Cu are 933 and 1358 K, respectively, but we use the values found by simulations, i.e., $T_m = 870$ K for Al^{43,44} and $T_m = 1327$ K for Cu.⁴⁵ One can see that in both metals the critical shear stress decreases with temperature almost linearly in a wide temperature range. In the normalized coordinates, the decrease rate is practically the same in Al and Cu. On the other hand, critical strain decreases with increasing temperature in a nonlinear fashion and the decrease in Cu is faster than in Al.

The linear decrease of critical stress with increasing temperature observed in our simulations is in line with the theory developed by Zhu *et al.* for dislocation nucleation from the surface.³³ According to their theory, at strain rates used in experiments, nucleation stress drops by more than 70% when temperature increases from 0 K to room temperature. For strain rates typical for MD simulations, the expected decrease is about 40%, while we observed a decrease of 25% for Al and 22% for Cu. This difference should be attributed to the absence of defects in our study. The critical stress of Al at 800 K is about 35% of that at 0 K, while the reduction in strength of Cu is about 50%.

The above-mentioned Frenkel's formula suggests $G/\tau_c = 2\pi$ for all crystalline materials. It is interesting to see how the ratio, G/τ_c , depends on temperature. The result is presented in Fig. 4, where it can be seen that for both metals the ratio increases with temperature almost linearly. The increase rate for Cu is somewhat higher than for Al. Since both G and τ_c

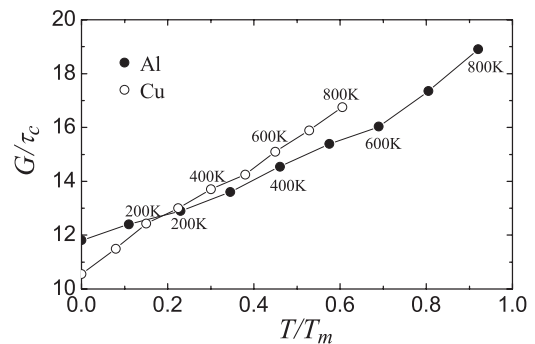


FIG. 4. Temperature dependence of the ratio G/τ_c for Al (filled circles) and Cu (open circles). Each point is the result of averaging over 10 numerical runs.

decrease with increasing temperature, the increase of the ratio, G/τ_c , means that τ_c drops with temperature faster than G . In the work of Ref. 20, a generalization of Frenkel's formula was offered in the form $G\gamma_c/\tau_c = \pi/2$, which incorporates the critical shear strain (shearability), γ_c . In Fig. 5, we present $G\gamma_c/\tau_c$ as a function of normalized temperature and reveal that this quantity is practically temperature-independent due to the nonlinear temperature dependence of γ_c . Indeed, the increase of temperature up to 800 K results in the increases of G/τ_c by 50%–60%, while $G\gamma_c/\tau_c$ varies within 10%.

According to our results, critical shear stress of Al and Cu at room temperature is about $\tau_c = 1.86$ GPa and $\tau_c = 2.24$ GPa, respectively, which may be compared to the values of critical resolved shear stress for dislocation nucleation that have been obtained in recent nanoindentation tests.^{5,46} Wang *et al.*⁴⁶ performed experiments with single crystals of Cu using different crystal orientations and indenter tips. Using the values of the reduced elastic modulus by Hertz's elastic theory,⁴⁷ the maximum shear stress can be estimated to be around 5.2 GPa in the case of indentation to a (111)-oriented surface, when one of the edges of the cube-corner indenter was parallel to $[11\bar{2}]$ direction. Minor *et al.*⁵ performed experiments on polycrystalline Al with a dislocation density of 10^{14} m⁻² to observe that most of the preexisting dislocations in indented grain escape to the surface in the early stage, followed by the so-called pop-in/load-drop effect that happens because of structural instability. They estimated the maximum shear stress right before the pop-in to be 2.3 GPa. The above-mentioned values of critical shear stress estimated from experimental data are higher than those predicted by our study, especially for Cu.

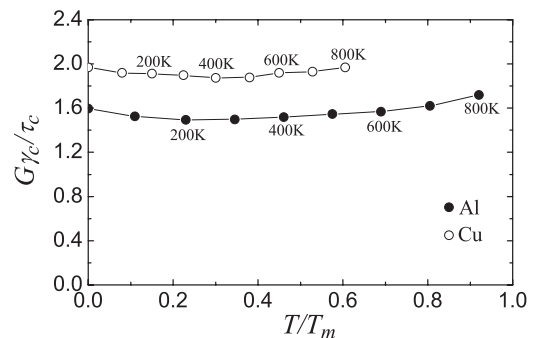


FIG. 5. Same as in Fig. 4, but for the quantity $G\gamma_c/\tau_c$.

We attribute this to the effect of the increase in the critical shear stress under superposed compressive stress reported by Ogata *et al.*, since material under the indenter tip is also compressed significantly.⁴² Ogata predicted up to two times larger critical stress when external normal stress is about 10 GPa, being of the same order of magnitude as normal stress induced by the indenter tip. Moreover, since all experimental values are accompanied by large scatter with about the order of 1 GPa, it can be stated that our results are in a reasonably good agreement with the experimental results.

To examine the atomistic mechanism of stacking fault formation, we have done an analysis of the structure factor defined as

$$S(x, z) = \left\langle \frac{1}{N_y} \left| \sum_j \exp(i\mathbf{TKr}_j) \right|^2 \right\rangle, \quad (1)$$

near the instability point. Here, $\mathbf{K} = (4\pi/a_0)(1, 0, 0)$ is the reciprocal lattice vector in the unstrained crystal, with a_0 being the lattice parameter, \mathbf{T} is the transformation matrix that takes into account strain and rotation of the deformed crystal, N_y is the number of atoms in the atomic row normal to the (x, z) plane, \mathbf{r}_j is the coordinate vector of the j th atom in the row, and i is the imaginary unit. If atoms sit on the points of a homogeneously deformed lattice, then the structure factor is $S = 1$. The deviation of atoms from the lattice points results in reduction of S . In Fig. 6, we present $S(x, z)$ in Cu at $T = 0$ K at the values of strain (a) $\gamma = 0.179$, (b) $\gamma = 0.182$, and (c) $\gamma = 0.185$. It can be seen that a static sinusoidal wave of displacements of very small amplitude ($\sim 10^{-4}$ Å) is formed prior to the stacking fault formation that occurs at the critical strain ($\gamma_c = 0.185$). Further loading transforms the sinusoidal modulation to the form of kink and the latter eventually triggers formation of the stacking fault at $\gamma = \gamma_c$. The wave of atomic displacements is observed not only at 0 K, but also at finite temperatures, though, for increasing temperature, loading should be done much slower to have enough time to average out thermal fluctuations.

No qualitative difference in the stacking fault formation mechanism was found between Al and Cu; therefore, we show only the results for Cu.

It should be pointed out that the scenario of crystal lattice instability presented above seems generic, as it has been observed in similar settings in other studies.^{18,19,48}

B. Cell size effect

The critical stress of Al, τ_c , under shear along $[11\bar{2}](111)$ is presented in Fig. 7 as a function of the number of atoms in the simulation cell, N , for different temperatures. For clarity, we present the results only for 10, 100, 200, 400, 600, and 800 K. Each point is the result of averaging over 10 MD runs. The scatter in the critical stress is shown by error bars. At 10 K, nearly the same value of 2.45 GPa was obtained for all studied N and negligible dispersion of τ_c was observed. However, already at 100 K, the critical stress estimated for the cells containing 48 and 162 atoms is noticeably lower than the value obtained with $N = 1296$. This means that tiny simulation cells can be used in MD simulations for the investigation of ISS only at very low temperatures.

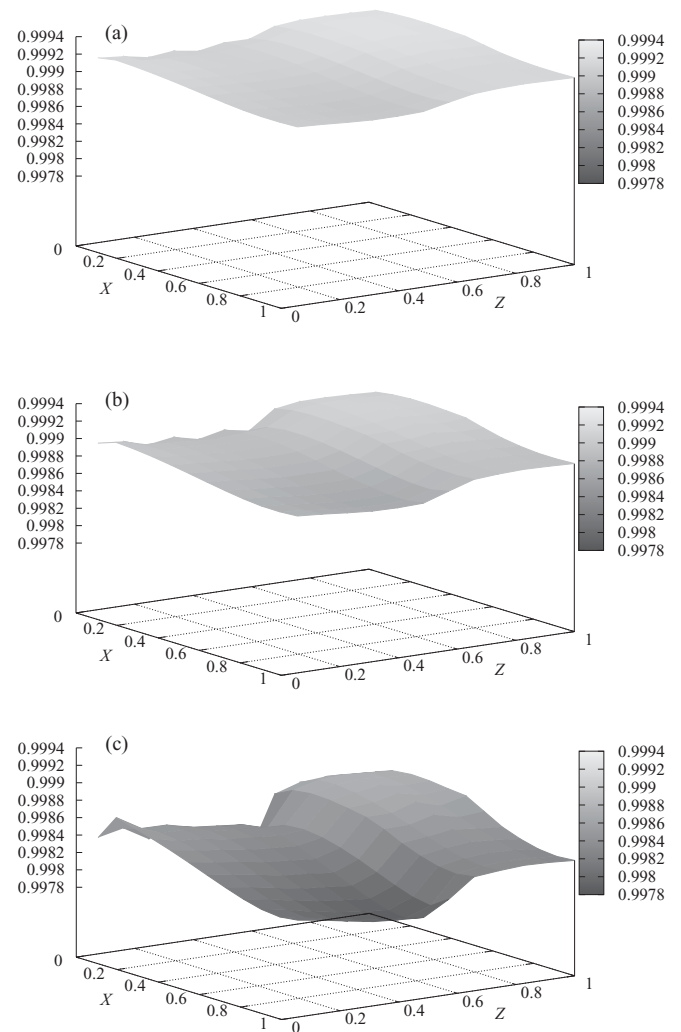


FIG. 6. Structure factor $S(x, z)$ calculated for Cu at $T = 0$ K at the values of strain (a) $\gamma = 0.179$, (b) $\gamma = 0.182$, and (c) $\gamma = 0.185$. The critical value of strain is $\gamma_c = 0.185$.

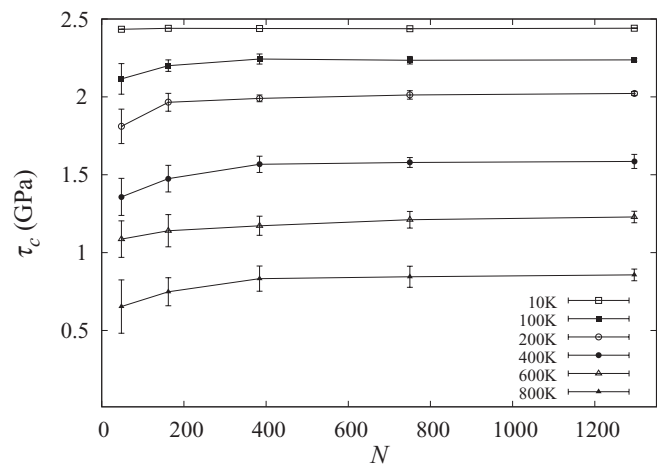


FIG. 7. Critical stress of Al, τ_c , under shear along $[11\bar{2}](111)$ as a function of the number of atoms in the simulation cell, N , for temperatures 10, 100, 200, 400, 600, and 800 K. Each point is the result of averaging over 10 numerical runs. The scatter in the critical stress is shown by the error bars.

In all cases, the results saturate and the dispersion of the results becomes relatively small at $N \sim 1000$. This implies that a simulation cell containing about 1000 atoms is large enough for the investigation of ISS even at high temperatures. It is worth noting that the scatter of critical stress depends on both the temperature and the cell size. It is therefore indispensable to average results over several runs at elevated temperatures, especially for small cells. The saturation of ideal stress for more than 750 atoms indicates that the application of *ab initio* calculation to investigation of ISS at high temperatures is difficult, considering that long-time simulation for each MD run is required.

The results obtained for Cu in the study of the cell size effect are very similar to those presented for Al, indicating that the aforementioned tendency of the size effect is general.

IV. CONCLUSIONS

MD simulations have been performed for investigating the effect of temperature on ideal shear strength of Al and Cu using EAM potentials. Gradually increasing shear stress was applied along the direction of the easiest sliding, $[11\bar{2}](111)$, until structural instability occurred. The temperatures up to 800 K were studied, which correspond to $0.9T_m$ for Al and $0.6T_m$ for Cu.

It was found that the elastic shear modulus, G , the critical shear stress, τ_c , and the critical shear strain, γ_c , decrease with increasing temperature. G and τ_c drop with temperature almost linearly, while γ_c also decreases with temperature, but in a nonlinear manner.

According to Frenkel's formula, the ratio, G/τ_c , is constant for all crystalline materials. Ogata *et al.*²⁰ have found that for a number of metals and ceramics the quantity, $G\gamma_c/\tau_c$, is indeed

nearly constant. Both these relations were obtained neglecting the temperature effect. We have found that for Al and Cu the ratio, G/τ_c , linearly increases with temperature and thus the decrease of τ_c with temperature is faster than that of G . On the other hand, $G\gamma_c/\tau_c$ was found to be almost temperature independent due to the nonlinear temperature dependence of γ_c . We believe that the temperature independence of the quantity $G\gamma_c/\tau_c$ is one of the main findings of the present work.

Our simulation results suggest that the critical shear stress of single crystals decreases slower with growing temperature than that of dislocation nucleation from surfaces. To be specific, for strain rates typical for MD simulations, Zhu *et al.*³³ predicted that the critical stress needed for dislocation nucleation from the surface at room temperature reduces by 40% compared to its value at 0 K. In our study of defect-free fcc metals, the reduction of ideal shear strength due to heating up to the room temperature is 25% for Al and 22% for Cu. This indicates that the temperature effect on the critical stress depends on structure.

Although empirical interatomic potentials do not produce quantitatively rigorous results, it seems to be difficult to employ *ab initio* calculations for the investigation of temperature effect on the ideal strength. This is because averaging over a number of MD runs with relatively large simulation cells (~ 1000 atoms) is required to evaluate critical stress and strain at finite temperature (≥ 100 K).

ACKNOWLEDGMENTS

The authors gratefully acknowledge the financial support provided by Japan Russia Youth Exchange Center and by the Russian Foundation for Basic Research, Grant No. 11-08-97057-p-povolzhie-a.

¹J. Frenkel, *Z. Phys.* **37**, 572 (1926).

²C. Herring and J. K. Galt, *Phys. Rev.* **85**, 1060 (1952).

³T. Zhu and J. Li, *Prog. Mater. Sci.* **55**, 710 (2010).

⁴B. Wu, A. Heidelberg, and J. J. Boland, *Nat. Mater.* **4**, 525 (2005).

⁵A. M. Minor, S. A. Syed Asif, Z. Shan, E. A. Stach, E. Cyrankowski, T. J. Wyrobek, and O. L. Warren, *Nat. Mater.* **5**, 697 (2006).

⁶M. Jahnátek, J. Hafner, and M. Krajčí, *Phys. Rev. B* **79**, 224103 (2009).

⁷D. Kiener, C. Motz, and G. Dehm, *Mater. Sci. Eng. A* **505**, 79 (2009).

⁸D. Kiener, W. Grosinger, G. Dehm, and R. Pippan, *Acta Mater.* **56**, 580 (2008).

⁹S. W. Lee, S. M. Han, and W. D. Nix, *Acta Mater.* **57**, 4404 (2009).

¹⁰Z. W. Shan, R. K. Mishra, S. A. Syed Asif, O. L. Warren, and A. M. Minor, *Nat. Mater.* **7**, 115 (2008).

¹¹A. T. Jennings, M. J. Burek, and J. R. Greer, *Phys. Rev. Lett.* **104**, 135503 (2010).

¹²G. Richter, K. Hillerich, D. S. Gianola, R. Monig, O. Kraft, and C. A. Volkert, *Nano Lett.* **9**, 3048 (2009).

¹³H. Bei, S. Shim, E. P. George, M. K. Miller, E. G. Herbert, and G. M. Pharr, *Scr. Mater.* **57**, 397 (2007).

¹⁴M. B. Lowry, D. Kiener, M. M. LeBlanc, C. Chisholm, J. N. Florando, J. W. Morris Jr., and A. M. Minor, *Acta Mater.* **58**, 5160 (2010).

¹⁵J. R. Morris, H. Bei, G. M. Pharr, and E. P. George, *Phys. Rev. Lett.* **106**, 165502 (2011).

¹⁶I. M. Mikhailovskij, T. I. Mazilova, V. N. Voyevodin, and A. A. Mazilov, *Phys. Rev. B* **83**, 134115 (2011).

¹⁷H. Bei, Y. F. Gao, S. Shim, E. P. George, and G. M. Pharr, *Phys. Rev. B* **77**, 060103(R) (2008).

¹⁸J. Li, K. J. Van Vliet, T. Zhu, S. Yip, and S. Suresh, *Nature (London)* **418**, 307 (2002).

¹⁹S. V. Dmitriev, J. Li, N. Yoshikawa, and Y. Shibutani, *Philos. Mag.* **85**, 2177 (2005).

²⁰S. Ogata, J. Li, N. Hirotsaki, Y. Shibutani, and S. Yip, *Phys. Rev. B* **70**, 104104 (2004).

²¹T. Tsuru, Y. Kaji, D. Matsunaka, and Y. Shibutani, *Phys. Rev. B* **82**, 024101 (2010).

²²R. Janisch, N. Ahmed, and A. Hartmaier, *Phys. Rev. B* **81**, 184108 (2010).

²³T. Tsuru and Y. Shibutani, *Phys. Rev. B* **75**, 035415 (2007).

- ²⁴K. Kolluri, M. R. Gungor, and D. Maroudas, *Phys. Rev. B* **78**, 195408 (2008).
- ²⁵K. Kolluri, M. R. Gungor, and D. Maroudas, *Appl. Phys. Lett.* **94**, 101911 (2009).
- ²⁶K. Kolluri, M. R. Gungor, and D. Maroudas, *J. Appl. Phys.* **105**, 093515 (2009).
- ²⁷Y. Umeno and M. Černý, *Phys. Rev. B* **77**, 100101(R) (2008).
- ²⁸Y. Umeno, Y. Shiihara, and N. Yoshikawa, *J. Phys. Condens. Matter* **23**, 385401 (2011).
- ²⁹M. Černý and J. Pokluda, *Comput. Mater. Sci.* **50**, 2257 (2011).
- ³⁰S. V. Dmitriev, T. Kitamura, J. Li, Y. Umeno, K. Yashiro, and N. Yoshikawa, *Acta Mater.* **53**, 1215 (2005).
- ³¹Y. Umeno, T. Shimada, and T. Kitamura, *Phys. Rev. B* **82**, 104108 (2010).
- ³²J. Li, *MRS Bull.* **32**, 151 (2007).
- ³³T. Zhu, J. Li, A. Samanta, A. Leach, and K. Gall, *Phys. Rev. Lett.* **100**, 025502 (2008).
- ³⁴M. Černý and J. Pokluda, *J. Phys. Condens. Matter* **21**, 145406 (2009).
- ³⁵K. Mizushima, S. Yip, and E. Kaxiras, *Phys. Rev. B* **50**, 14952 (1994).
- ³⁶R. D. Boyer, J. Li, S. Ogata, and S. Yip, *Modell. Simul. Mater. Sci. Eng.* **12**, 1017 (2004).
- ³⁷Y. Mishin, D. Farkas, M. J. Mehl, and D. A. Papaconstantopoulos, *Phys. Rev. B* **59**, 3393 (1999).
- ³⁸R. R. Zope and Y. Mishin, *Phys. Rev. B* **68**, 024102 (2003).
- ³⁹M. Parrinello and A. Rahman, *J. Appl. Phys.* **52**, 7182 (1981).
- ⁴⁰A. M. Iskandarov, S. V. Dmitriev, and Y. Umeno, *J. Solid Mech. Mater. Eng.* (to be published).
- ⁴¹LAMMPS 2011 [<http://lammps.sandia.gov/>].
- ⁴²S. Ogata, J. Li, and S. Yip, *Science* **298**, 807 (2002).
- ⁴³J. Wang, A. Horsfield, P. D. Lee, and P. Brommer, *Phys. Rev. B* **82**, 144203 (2010).
- ⁴⁴A. S. Lopis, Q. G. Reynolds, and K. Bisaka, paper presented at the Conference of Metallurgistics, Vancouver, 2010 (unpublished).
- ⁴⁵A. Suzuki and Y. Mishin, *J. Mater. Sci.* **40**, 3155 (2005).
- ⁴⁶W. Wang and K. Lu, *Philos. Mag.* **86**, 5309 (2006).
- ⁴⁷K. L. Johnson, *Contact Mechanics* (Cambridge University Press, New York, 1996).
- ⁴⁸A. A. Ovcharov, S. V. Dmitriev, and M. D. Starostenkov, *Comput. Mater. Sci.* **9**, 325 (1998); S. V. Dmitriev, A. A. Ovcharov, M. D. Starostenkov, and E. V. Kozlov, *Phys. Solid State* **36**, 996 (1996).